Theoretical Investigation of the Interaction between Fluorinated Dimethyl Ethers ($n_F = 1-5$) and Water: Role of the Acidity and Basicity on the Competition between OH···O and CH···O Hydrogen Bonds

Salma Parveen and Asit K. Chandra*

Department of Chemistry, North Eastern Hill University, Shillong 793022, India

Thérèse Zeegers-Huyskens*

Department of Chemistry, University of Leuven, Leuven, B-3001, Belgium

Received: March 13, 2009; Revised Manuscript Received: April 8, 2009

Theoretical calculations have been carried out using ab initio MP2 and B3LYP density functional methods to investigate the interaction between fluorinated dimethyl ethers ($n_F = 1-5$) and water. Depending on the number of F atoms implanted on the dimethyl ethers, linear structures stabilized by intermolecular O_wH_w···O or CH···O_w hydrogen bonds or closed structures involving both hydrogen bonds are formed. Binding energies of the hydrogen-bonded complexes range between 4 and 12 kJ mol^{-1}. Blue shifts of the CH stretching vibrations are predicted even in the absence of a direct CH···O interaction. The red shifts of the OH stretching vibrations of water in the open and closed structures are analyzed as well. The natural bond orbital analysis includes the $\sigma^*(O_wH_w)$ and σ^*(CH) occupation, the hybridization of the C atom, the atomic charges, and the intra- and intermolecular hyperconjugation energies. These parameters are discussed as a function of the proton affinity (PA) of the O atom and the deprotonation enthalpy (DPE) of the CH bonds of the fluorinated ethers calculated in a previous work.[16] Our results show that the effective PA in determining the intermolecular O → $\sigma^*(O_wH_w)$ hyperconjugation energies decreases with increasing acidity of the CH bond. In turn, the effective acidity of the CH bond in determining the intermolecular O_w → σ^*(CH) hyperconjugation energies decreases with increasing basicity of the O atom.

Introduction

Hydrogen bonding (HB) is one of the most important noncovalent interactions and it plays a crucial role in understanding many chemical and biological processes, such as arrangement of molecules in crystals, controls in biochemical processes, stabilization of macromolecules, and so forth.[1−3] Hydrogen-bonded complexes play an important role in climate change as well.[4] The formation of a hydrogen bond X−H···Y results from the interaction between a proton donor X−H and a proton acceptor Y bearing lone pair(s) or π-deficient systems. One of the characteristic features of classical hydrogen bonds is the X−H bond lengthening with a concomitant red shift and infrared intensity increase of the X−H stretching vibration. These spectroscopic features are observed in the great majority of complexes involving polar O−H or N−H groups. However, experimental and theoretical studies have reported the existence of blue-shifted hydrogen bonds in which hydrogen-bond formation leads to X−H (mainly CH) bond shortening and, most of the time, an infrared intensity decrease of this vibration. This past decade, these blue shifts received much attention from theoreticians[5] and experimentalists.[6] Whereas some patterns begin to emerge, there are not yet any accepted rules that allow us to predict whether a given CH bond shifts to the red or blue. Most of the studies have concluded that there is no fundamental distinction between blue- and red-shifted hydrogen bonds.[7] Briefly summarizing, let us say that following the rehybridization/hyperconjugation mechanism, the C−H bond length should be controlled by two main factors acting in opposite directions, namely the X−H bond lengthening due to an increase of the occupation of the σ^*(C−H) orbital by hyperconjugation and the X−H bond shortening due to an increase in the *s*-character of the X atom of the X−H bond.[8] Further, a necessary condition for a proton donor A−H to form a blue-shifting H-bond should be the presence of a negative dipole moment derivative with respect to the stretching coordinate. [9] In a recent paper, a large number of blue-shifted H-bonded systems has been examined and it has been concluded that the predominance of repulsive or attractive forces results in a shortening or lengthening of the group involved in hydrogen-bond formation.[10] Interestingly, a recent study on geometric isotope effects on various intermolecular and intramolecular C−H···O hydrogen bonds has demonstrated that these hydrogen bonds can be categorized as typical hydrogen bonds.[11]

Further, blue shifts can also occur at those C−H groups that do not participate directly in hydrogen-bond formation. This effect has been observed experimentally for several decades[12,13] and is referred to as the "lone-pair effect" resulting from back-donation of electronic charge from the lone pair(s) to the antibonding σ^*(C−H) orbital of the C−H bond in gauche conformation with respect to the lone pair(s).[14] This effect has been discussed in recent works.[15]

In the present work, the interaction between dimethyl ether (DME) and fluorinated dimethyl ethers (FDMEs, $n_F = 1$ to 5) and water is investigated. Fluorinated ethers can have different conformations and the main factor governing the conformation is the hyperconjugative effect taking place from the lone pairs of the oxygen atom to the σ^*(CH) or σ^*(CF) antibonding

* To whom correspondence should be addressed. E-mail: akchandra@nehu.ac.in. E-mail: therese.zeegers @chem.kuleuven.be.

10.1021/jp902244j CCC: $40.75
Published on Web 05/07/2009

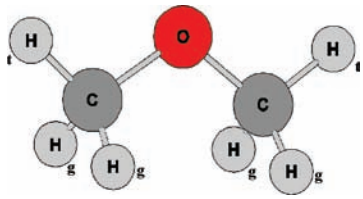

Figure 1. CH^t and CH^g bonds in dimethyl ether derivatives.

orbitals in gauche position (Figure 1).[16] A good method to investigate this effect is to study the interaction with proton donors, the lone pair(s) of the O atom being partially involved in the formation of a hydrogen bond. Several experimental and theoretical works have shown that DME can act as a proton acceptor.[17] This molecule can also act as a weak proton donor and this has been suggested by the fact that it is able to form dimers where the two molecules are held together through CH···O hydrogen bonds.[8] As shown in a recent theoretical work,[16] fluorine substitution strongly decreases the proton acceptor ability of the O atom and increases the acidity of the C−H bonds. The OH bond of water can act as a proton donor and its O atom as a proton acceptor. Therefore, it seemed to us interesting to discuss to what extent the acidity and basicity of FDMEs influence the formation of OH···O or CH···O hydrogen bonds.

The present work is arranged as follows. In the first part, the structure and binding energies are discussed. The second part deals with the variation of the distances and vibrational frequencies. In the last part, the results of a natural bond orbital analysis are presented.

Computational Methods

The geometries of isolated DME and symmetric as well as asymmetric substituted fluorinated ethers ($F_nH_{3-n}COCF_mH_{3-m}$, $n = 0-3$ and $m = 1-2$) and their hydrogen-bonded complexes with H_2O were fully optimized by using the MP2 and B3LYP[19] methods combined with the 6-311++G(d,p) basis set. Harmonic frequency calculations were carried out at the same level to characterize the stationary points. The vibrational frequencies were retained unscaled, as our main interest is not to calculate the accurate frequencies but the frequency shifts due to hydrogen bonding. It should be pointed out that the fluorinated ethers can have several conformations, but only the lowest energy conformer was considered here. Charges on individual atoms, hybridization, orbital occupancies, and hyperconjugative energies were obtained by the natural bond orbital (NBO) population scheme,[20] using the B3LYP/6-311++G(d,p) method and the MP2 optimized geometries. We could not perform NBO analysis at the MP2 level because of a technical problem in *Gaussian 03* program. Because B3LYP and MP2 results do not differ significantly, we believe that our NBO analysis is consistent and reliable. The hydrogen-bonding energies ($-\Delta E_{HB}$) of the complexes were calculated from the energy difference between the complexes and the monomers. The calculated $-\Delta E_{HB}$ values include the zero-point energy (ZPE) correction and the basis set superposition error (BSSE) computed by the counterpoise (CP) method.[21] The *Gaussian 03* package was used for all of the calculations analyzed in the present work.[22]

Results and Discussion

1. Optimized Geometries and Binding Energies of the FDMEs−H_2O Complexes. Several stable structures are found on the potential energy surface (PES) of the FDMEs−H_2O complexes. These structures are illustrated in Figure 1 that also indicates the structure of the DME−H_2O complex useful for the comparison. This complex is characterized by a quasi-linear $O_wH_w\cdots O_1$ hydrogen bond. We note that the intermolecular distance of 1.86 Å is practically the same as the distance of 1.87 Å calculated at the MP2/6-311++G(2d,2p) level.[23] In the $CH_3OCH_2F\cdot H_2O$ complex, the intermolecular distance of 1.920 Å is longer than in the $DME\cdot H_2O$ complex. There is a departure from linearity, the $O_wH_w\cdots O$ angle being 163.2°. No classical hydrogen bond is formed between the C3H8 group and the O_w atom, the $H8\cdots O_w$ distance being as long as 3.071 Å. However, the $O_wH_w\cdots O$ angle is smaller in the $CH_3OCH_2F\cdot H_2O$ complex (163.2°) than in the $CH_3OCH_3\cdot H_2O$ one (172.6°), which may suggest a weak electrostatic interaction between the O_w and H8 atoms. In the $CHF_2OCF_3^-\cdot H_2O$ complex, one stable linear structure stabilized by a linear $CH\cdots O_w$ hydrogen bond is found on the potential energy surface (PES). For the other FDMEs containing 2, 3, or 4 F atoms, the most stable structures of the H_2O complexes are cyclic and characterized by $O_wH_w\cdots O1$ and $CH\cdots O_w$ hydrogen bonds.

It must be noted here that MP2/6-311++G(2d,2p) calculations have revealed two different structures between DME and H_2O_2. The most stable structure is cyclic and is characterized by OH···O and CH···O hydrogen bonds.[24] We were not able to find this type of structure for the DME−H_2O complex. Our calculations indicate that the intermolecular distances $H_w\cdots O1$ increase from 1.860 to 2.269 Å and that the intermolecular $O_wH_w\cdots O1$ angles decrease from 173 to 120° on going from the $DME\cdot H_2O$ to the $CH_2FOCF_3\cdot H_2O$ systems, indicating a decrease of the $O_wH_w\cdots O1$ hydrogen-bond strength with the increase in number of F atoms. Inversely, the intermolecular $H\cdots O_w$ distances decrease and the $CH\cdots O_w$ angles slightly increase with the number of F atoms, indicating a strengthening of the $CH\cdots O_w$ hydrogen bond with increasing F substitution. Comparison of the structures of the complexes between CHF_3 and FDMEs is interesting. It has indeed been shown that, at the potential energy minimum, the O atom acts as a proton acceptor. For the complex between CH_3OCF_3 and CHF_3, the CH bond of CHF_3 lies between the F and O atoms of the ether derivative and, in the CF_3OCF_3 complex, the ether O atom does not act as a proton donor.[17c]

Our calculations indicate that for CH_2FOCH_2F, CH_3OCHF_2, and CH_2FOCHF_2 complexes with H_2O, linear $CH\cdots O_w$ complexes are also stable on the PES, although less stable than the closed ones. It must be mentioned here that other stable structures involving bifurcated (CH···O···HC) or CH···F hydrogen bonds are also found on the PES. These structures and the corresponding binding energies are given in SI.1 of the Supporting Information and will no more be discussed hereafter.

Table 1 contains the binding energies of the studied complexes calculated with the MP2 and B3LYP methods. Both methods show the same trend; the B3LYP binding energies for the linear complexes are however higher than the MP2 ones. In the further discussion, we will consider the MP2 energies only. Table 1 also reports the proton affinity (PA) of the O atoms and the deprotonation enthalpy (DPE) of the CH bonds involved in the interaction with H_2O, which have been calculated in a previous work.[16] It must be mentioned here that the PA of the O atom decreases regularly with the number of F atoms implanted on the FDMEs. This is not the case for the DPE of the CH groups, the DPE being lower for the CH^g than for the CH^t groups. The DPEs of the CH groups are larger for the FDMEs bearing a CF_3 group. When $F = 3$ for example, the PAs of CH_3OCF_3 and CH_2FOCHF_2 are about the same (665 kJ mol^{-1}) but their DPEs differ markedly, being 1633 kJ mol^{-1}

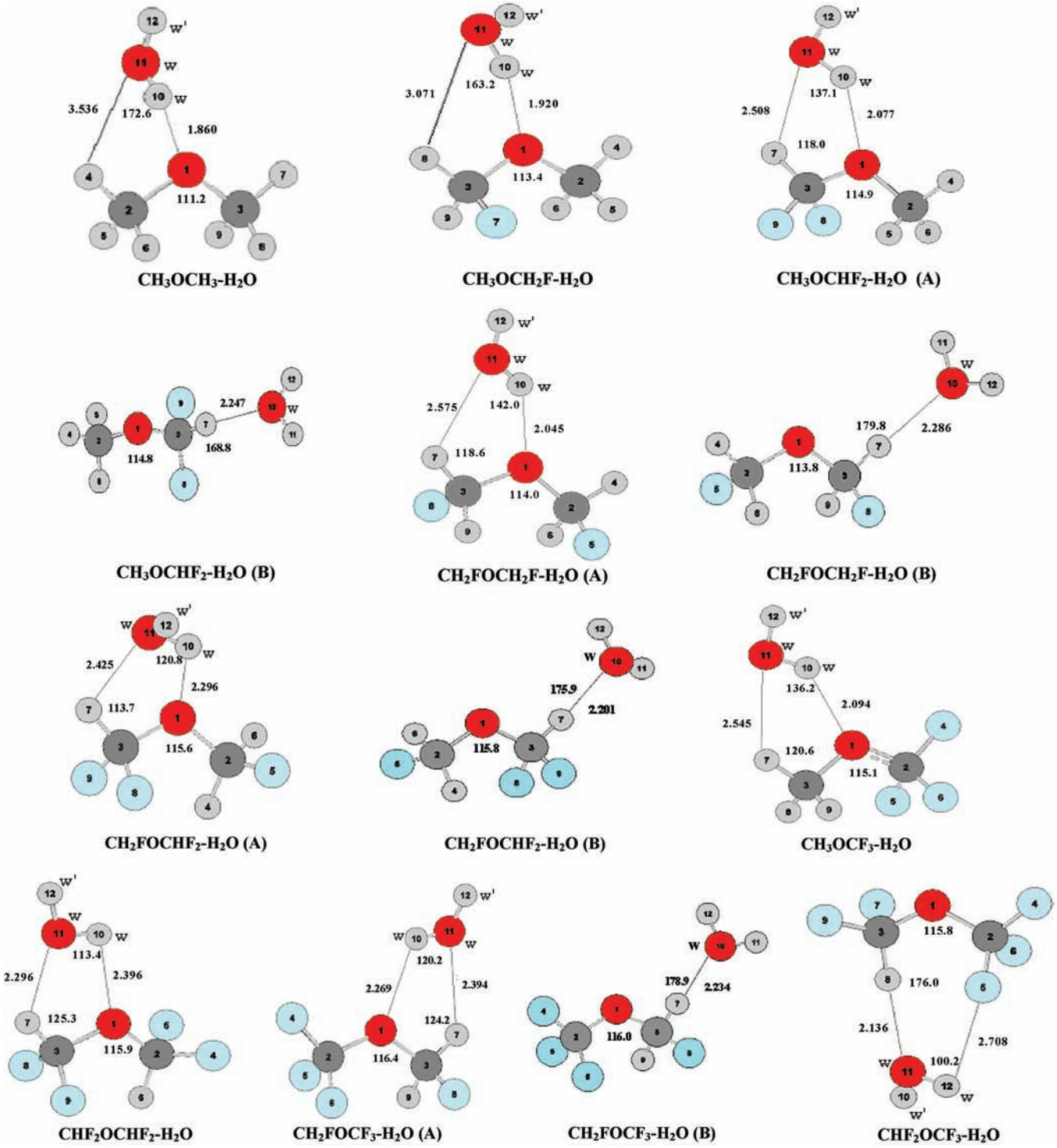

Figure 2. MP2/6-311++G(d,p) optimized geometries of DME and FDMEs complexed with one H_2O molecule.

for the first molecule and 1572 kJ mol^{-1} for the second one. These differences are important for the further discussion. Our results show that the binding energies of the most stable complexes range between −7.7 and −12.4 kJ mol^{-1} (MP2 calculations). The data can be discussed as a function of the acidities or basicities of the groups involved in the interaction. When the PA of the oxygen atom of the ether derivative is equal to 743 kJ mol^{-1} or larger and when the DPE of the CH bond is equal to 1678 kJ mol^{-1} or larger, the complexes are formed preferentially on the O atom. It must be remembered that the PA(O) of water is 691 kJ mol^{-1} and the DPE of the OH bond is equal to 1633 kJ mol^{-1}. [25] Thus, the basicity of water is lower and the acidity of water is higher than those of DME and its monofluorinated derivative. Further, when both the PA of the O atom (608 kJ mol^{-1}) and the DPE of the CH bond (1504 kJ mol^{-1}) are low, CH···O hydrogen bond is preferred over the OH···O one. In this case, water is less acidic and more basic than CHF_2OCF_3. When the PA(O) values range between 635 and 708 kJ mol^{-1} and the DPE(CH) values range between 1534 and 1635 kJ mol^{-1}, cyclic hydrogen-bonded structures are preferred over the linear ones. As illustrated in Figure 3, there is for the most stable complexes an inverse correlation between the CH···O_w and O_wH_w···O1 intermolecular distances, indicating that, when the CH···O_w hydrogen bonds become stronger,

TABLE 1: Hydrogen-Bond Energies ($-\Delta E_{HB}$) of the Complexes between DMFEs and H_2O Calculated at the MP2 (Full) and B3LYP Levels with the 6-311++G(d,p) Basis Set; Proton Affinity of the Oxygen Atom [PA(O)] and Deprotonation Enthalpy for the CH Bond [DPE(CH)] Involved in Hydrogen Bond Formation[a]

System	$-\Delta E_{HB}$[b]		PA(O)[b]	DPE(CH)[c]
	MP2	B3LYP		
$CH_3OCH_3-H_2O$	12.4 (8.4, 8.4)	14.2 (7.9, 2.6)	791.0	1717.6
$CH_3OCH_2F-H_2O$	10.1 (6.8, 6.9)	10.7 (6.5, 2.2)	743.5	1677.8
$CH_2FOCH_2F-H_2O$ (A)	7.7 (6.2, 6.5)	7.9 (6.1, 1.3)	703.8	1635.4
$CH_2FOCH_2F-H_2O$ (B)	4.1 (4.2, 5.4)	5.8 (3.7, 1.5)		
$CH_3OCHF_2-H_2O$ (A)	8.0 (6.2, 6.5)	7.3 (6.0, 2.2)	707.7	1611.2
$CH_3OCHF_2-H_2O$ (B)	5.1 (4.1, 6.0)	7.5 (3.7, 1.2)		
$CH_2FOCHF_2-H_2O$ (A)	8.8 (5.3, 7.3)	7.9 (5.7, 2.4)	666.3	1572.1
$CH_2FOCHF_2-H_2O$ (B)	7.5 (4.2, 6.3)	8.7 (3.9, 2.6)		
$CH_3OCF_3-H_2O$	8.7 (5.9, 6.6)	9.2 (5.8, 0.9)	665.2	1633.4
$CHF_2OCHF_2-H_2O$	11.1 (5.5, 7.3)	11.0 (4.8, 2.4)	645.0	1534.1
$CH_2FOCF_3-H_2O$ (A)	8.9 (5.5, 6.9)	7.9 (5.5, 2.3)	634.6	1589.0
$CH_2FOCF_3-H_2O$ (B)	7.3 (4.4, 5.9)	8.4 (4.2, 2,5)		
$CHF_2OCF_3-H_2O$	11.0 (5.1, 9.3)	12.6 (4.3, 3.3)	608.2[c]	1503.9

[a] Data are in kJ mol^{-1}. [b] The first entries correspond to the binding energies with ZPE- and BSSE-corrections; the ZPE- and BSSE-corrections are indicated in parentheses. [c] Ref 16; the DPE was erroneously indicated as 643.6 kJ mol^{-1} instead of 608.2 kJ mol^{-1}.

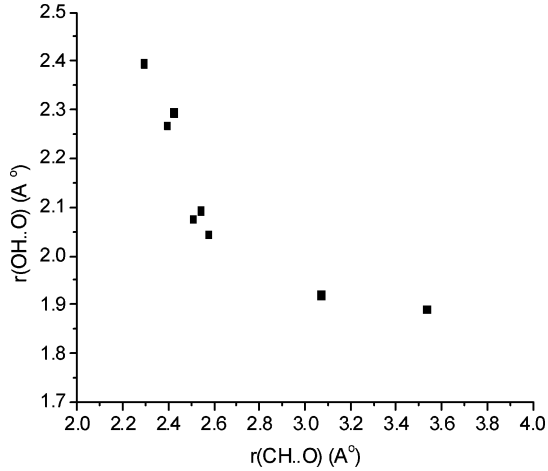

Figure 3. $r(CH\cdots O_w)$ as a function of $r(O_wH_w\cdots O1)$ (Å).

the $O_wH_w\cdots O1$ hydrogen bonds become weaker. For the five linear $CH\cdots O_w$ complexes, the lowest binding energy (−4.1 kJ mol^{-1}) is predicted for the $CH_2FOCH_2F\cdot H_2O$ complex and the largest binding energy (−11.0 kJ mol^{-1}) is calculated for the CHF_2OCF_3 complex. This is in agreement with the DPE values of the corresponding CH bonds equal to 1635 and 1504 kJ mol^{-1}, respectively. For the five linear $CH\cdots O_w$ complexes, the binding energies are linearly correlated to the acidity of the CH bonds. For the closed complexes, no correlation between PA and DPE could be found. This may be accounted for by the fact that, as previously mentioned, the intermolecular $O_wH_w\cdots O1$ and $CH\cdots O_w$ angles vary within a broad range. A correlation between hydrogen-bond energies and proton donor/proton acceptor abilities was found in closed complexes involving nucleobases and water only when the intramolecular angles vary within a small range.[26]

2. Variations of the CH and OH Distances and the ν(OH) Frequencies and IR Intensities. Table 2 reports the CH distances in isolated FDMEs in the water complexes along with the variation of the CH distances resulting from the interaction with water. The C1O3 distances increase by a nearly constant value of 7−9 mÅ in all of the structures and will no more be discussed hereafter. A first remark concerns the CH distances in isolated FDMEs. As shown by the results reported in Table 2, in isolated DME, the C2H5 and C2H6 distances (CH^g) are longer than the C2H4 (CH^t) one. These differences have been assigned to the anomeric effect resulting from a negative hyperconjugation between the lone-pair orbital of the O atom to the σ^*(CH) orbital, which is larger for the two CH bonds in gauche position.[27] Let us mention that the anomeric effect has been discussed for other FDMEs or hydrofluoro-ethers as well.[28]

As previously stated, an indirect way to examine the anomeric effect is to introduce a reagent that will interact with the O atom. In the hydrogen-bond complexes between DME and water or fluoroform, one of the O lone pairs of the ether molecule is involved in the OH···O or the CH···O hydrogen bond. This interaction results in small experimental blue shifts between 8 and 12 cm^{-1} of the $\nu(CH_3)$ stretching vibration.[17] Our calculations show that the CH^t bond is shortened by 0.4 mÅ and that the two other CH bonds are shortened by 2 and 2.1 mÅ. Note that our calculations are in good agreement with MP2/6-311++G(2d, 2p) calculations predicting CH bond shortenings of 0.4, 1.7, and 2.0 mÅ.[23] The same trend is predicted for the $CH_3OCH_2F\cdot H_2O$ complex. The closed complexes show a contrasting behavior. In these structures, the contraction of the C3H7 bond involved in the $CH\cdots O_w$ interaction takes values between 0.7 and 2.2 mÅ, whereas the variation of the other CH distances is smaller, being comprised between −0.4 and 0.4 mÅ. In the linear structures (B) or in the $CHF_2OCF_3\cdot H_2O$ complex, there is a contraction of the CH bond involved in the $CH\cdots O_w$ interaction by 1.6 to 2.2 mÅ. Our results indicate that, with the exception of the $CH_3OCH_3\cdot H_2O$ complex, the magnitude of the nonbridging CH contraction is smaller than the contraction of the bridging CH···O bond. There is no relation between the binding energies and the changes in the CH distances, the most stable $CHF_2OCF_3\cdot H_2O$ complex being characterized by the smallest contraction of the CH bond. The other CH bonds in the open structures remain almost unchanged. These characteristics will be discussed more in detail in the next section.

Our calculations predict six ν(CH) stretching modes in isolated DME. The two a1 modes are predicted at 3291 and 3033 cm^{-1}, the two b2 modes at 3190 and 3025 cm^{-1}, the a2 mode at 3096 cm^{-1}, and the b1 mode at 3090 cm^{-1}. Interaction with water results in blue shifts of these six fundamental modes, the a2 and b1 modes are shifted by 31 and 29 cm^{-1} respectively, whereas the high-frequency a1 and b2 modes being shifted by 8 and 9 cm^{-1}, respectively. The IR intensities of the six modes decrease. These data are in good agreement with literature results.[23] To have a best estimation of the frequency shifts of

TABLE 2: CH Distances (Å) in Isolated FDMEs (r°) and in Their Water Complexes (r^c)(Å) and Changes Resulting from the Interaction with Water (mÅ) (the CH Bonds in Bold Characters Indicate the CH Bond Involved in the H-Bond Interaction); Results from MP2/6-311++G(d,p) Calculations

bond	r°(CH)	r°(CH)	Δr(CH)
CH_3OCH_3			
C2−H4	1.0901	1.0897	−0.4
C2−H5	1.0991	1.0971	−2
CH_3OCH_2F			
C2−H4	1.0885	1.0886	0.1
C2−H6	1.0968	1.0956	−1.2
C3−H9	1.0968	1.0954	−1.4
$CH_2FOCH_2F(A)$			
C2−H4	1.0874	1.0878	0.4
C2−H6	1.0914	1.0912	−0.4
C3H7	1.0874	1.0867	−0.7
C3−H9	1.0914	1.0909	−0.5
$CH_2FOCH_2F(B)$			
C3H7	1.0874	1.0853	−2.1
C3H9	1.0914	1.0916	0.2
$CH_3OCHF_2(A)$			
C2H4	1.0872	1.0875	0.3
C2H5	1.0909	1.0905	−0.4
C3H7	1.0867	1.0858	−0.9
$CH_3OCHF_2(B)$			
C3−H7	1.0867	1.0845	−2.2
CH_3OCF_3			
C3H7	1.0867	1.0865	−0.2
C3H8	1.0907	1.0903	−0.4
$CH_2FOCCHF_2(A)$			
C2H4	1.0899	1.0896	−0.3
C2−H6	1.0875	1.0879	0.4
C3−H7	1.0862	1.0840	−2.2
$CH_2FOCHF_2(B)$			
C3−H7	1.0862	1.0843	−1.9
CHF_2OCHF_2			
C2H6	1.0881	1.0876	−0.5
C3−H7	1.0855	1.0836	−1.9
$CH_2FOCF_3(A)$			
C3H7	1.0869	1.0854	−1.5
C3H9	1.0903	1.0899	−0.4
$CH_2FOCF_3(B)$			
C3H7	1.0869	1.0850	−1.9
CHF_2OCF_3			
C3H8	1.0890	1.0874	−1.6

the individual CH groups, we have calculated the vibrational frequencies and IR intensities in the partially substituted isotopomers. For each complex, two isotopomers are considered. In isolated CH4D5D6OCD$_3$, for example, the ν(C2H4) vibration is predicted at 3180 cm^{-1} and, in the H_2O complex, this vibration is calculated at 3186 cm^{-1}, giving a shift of 6 cm^{-1}. In isolated CD4H5D6OCD$_3$, the ν(C2H5) vibration is calculated at 3072 cm^{-1}; this vibration is blue-shifted by 26 cm^{-1} in the complex. These data are in agreement with the shortening of the C2H4 and C2H5 bonds. Further, both vibrations are characterized by a decrease in the IR intensity as predicted or observed for most of the blue-shifted CH groups[5,6] but, as observed for several systems, this decrease does not correlate with the frequency shifts. Table 3 reports the frequencies calculated in the other isotopomers and their water complexes. Large blue shifts of 32 to 38 cm^{-1} are calculated for the CH···O$_w$ bonds in the linear B complexes. These shifts are consistent with the large contraction of the CH bonds in the linear CH···O$_w$ bonds.

A linear correlation is obtained between the change in CH bond length (mÅ) and the shift of the corresponding ν(CH) vibration (cm^{-1}):

$$\Delta r(\mathrm{CH}) = 0.06 - 0.062\Delta\nu(\mathrm{CH}) \quad (r = 0.980) \quad (1)$$

It must be mentioned that the slope of this correlation does not markedly differ from the slope of −0.056 obtained for the CH···O$_w$ hydrogen bonds in complexes involving halogenomethanes and water.[5i]

Complex formation between FDMEs and H_2O also results in variation of the OH distances and ν(OH) vibrational frequencies and IR intensities. The data are summarized in Table 4. In the linear (B) complexes, the interaction with water induces very small perturbations of the r(OH) distances (1 mÅ) and the ν(OH) vibrational frequencies (10 cm^{-1}). It must be remembered here that, when water acts as a proton donor toward a given base, the ν^s(OH) vibration can be considered, in a first approximation, as the vibration of the bonded OH group.[29] As expected, the elongation of the OH bond and the frequency shift of the ν^s(OH) vibration are the largest for the DME·H_2O and CH_3OCH_2F·H_2O complexes. These two parameters decrease further with the number of F atoms. The following linear correlation between the variation of the OH distances (mÅ) and the frequency shifts (cm^{-1}) is obtained:

$$\Delta r(\mathrm{OH}) = 0.44 - 0.097\Delta\nu(\mathrm{OH}) \quad (r = 0.991) \quad (2)$$

where $\Delta\nu$(OH) is the shift calculated from the average of the two ν(OH) vibrations. The variation of the IR intensities of the ν^{as}(OH) and ν^s(OH) vibrations is also worth mentioning. In isolated water, the ratio of the IR intensities (ν^{as}(OH)/ν^s(OH) is equal to 5.2. In the DME·H_2O and CH_3OCH_2F·H_2O complexes, the IR intensity of the ν^{as}(OH) vibration is markedly lower than that of the ν^s(OH) vibration, the ratios of the intensities being 0.22 and 0.44, respectively. This is the usual behavior when one of the OH bonds of water is involved in hydrogen-bond formation.[29] The reverse holds for the other cyclic complexes, the intensity ratio (ν^{as}(OH)/ν^s(OH) being comprised between 1.3 and 5.1. An increase of this ratio is related to a decrease of the participation of the O$_w$H$_w$···O1 bond in the closed structures.

3. NBO Analysis. Table 5 lists the σ^*(CH) occupation for relevant CH bonds in the isolated and complexed FDMEs along the change in hybridization of the C at the H. This table also indicates the change in the σ^*(O$_w$H$_w$) occupation in the most stable complexes. In the linear complexes, the change of the σ^*(O$_w$H$_w$) occupation is negligible. In Table 6, the variations of intramolecular hyperconjugation resulting from the interaction with water are reported. This table also indicates the intermolecular hyperconjugation energies taking place from the two lone pairs of the O1 atom to the σ^*(O$_w$H$_w$) orbitals along with the hyperconjugation energies from the lone pair(s) of the O$_w$ of H_2O to the relevant σ^*(CH) orbital. This table also reports the overall charge transfer taking place from the water molecule to the FDMEs along with the difference between the NBO charges on the H$_w$ and H$_{w'}$ atoms (qH$_w$ − qH$_{w'}$). NBO charges on all the atoms can be obtained in SI.2 of the Supporting Information.

We will consider at first the NBO properties of the bonded H_2O molecule. As outlined in the previous section, the lengthening of the O$_w$H$_w$ bond in the O$_w$H$_w$···O1 hydrogen bond ranges from 1.2 mÅ (CHF_2OCF_3) to 9.8 mÅ (CH_3OCH_3) (Table 4). This lengthening is mainly determined by the change in occupation of the σ^*(O$_w$H$_w$) orbital, which ranges from 0.2 to 20.4 me for the considered systems.

We obtained the following linear correlation:

$$\Delta r(O_wH_w) = 0.37\Delta\sigma^*(O_wH_w) + 1.43 \quad (r = 0.986) \tag{3}$$

where the elongation of the O_wH_w is expressed in mÅ and the increase in $\sigma^*(O_wH_w)$ occupation in me.

Further, the LPO1 → $\sigma^*(O_wH_w)$ second-order hyperconjugation energies markedly increase, from 1 to 37.7 kJ mol^{-1}, on going from the CHF_2OCHF_2 to the CH_3OCH_3 complexes. Figure 4 illustrates the linear correlation between the elongation of the O_wH_w bond (mÅ) and the $E^{(2)}$ [(LPO1 → $\sigma^*(O_wH_w)$] hyperconjugation energies (kJ mol^{-1})

$$\Delta r(O_wH_w) = 0.207[E^{(2)}(\text{LPO1}) \rightarrow \sigma^*(O_wH_w)] + 1.87 \quad (r = 0.987) \tag{4}$$

As outlined in section 1, we were not able to find a correlation between the hydrogen-bond energies and the acidity or basicity of the centers involved in the interaction. However, it may be interesting to look at the influence of the PA or DPE of the FDMEs on the properties of the individual O_wH_w···O1 or CH···O_w hydrogen bonds in the cyclic structures.

Comparison of the data of Tables 1 and 6 shows that there is a very rough correlation between the intermolecular $E^{(2)}$ [LPO1 → $\sigma^*(O_wH_w)$] energies and the PA values of the FDMEs but a great dispersion of the points is observed for low PA values, ranging between 640 and 710 kJ mol^{-1}. A closer inspection of our data allows one to obtain a better correlation when considering also the acidity of the CH bonds involved in the interaction. The CH_3OCF_3 and CH_2FOCHF_2 molecules are characterized by about the same PA (665 and 666 kJ mol^{-1}, respectively) and the intermolecular hyperconjugation energy is larger for the first complex (7.3 kJ mol^{-1}) than for the second one (1.7 kJ mol^{-1}). This may be accounted for by the larger DPE of the first molecule (1633 kJ mol^{-1}) as compared with the second one (1572 kJ mol^{-1}). These results suggest that the *effective* PA of the O1 atom decreases (from its actual PA value) with increasing proton donor ability of the CH group. This can be expressed by the following second-order polynomial illustrated in Figure 5:

$$E^{(2)}[(\text{LPO1}) \rightarrow \sigma^*(O_wH_w)] = (3 \times 10^{-4})X^2 - 0.23X + 47.4 \quad (r = 0.999) \tag{5}$$

where X = (PA − ΔDPE), ΔDPE being the difference in DPE of CH_3OCH_3 taken as a reference and the considered FDMEs. Let us mention that several nonlinear equations between hydrogen-bond properties and PAs have been derived.[30]

In the next step, we will discuss the NBO parameters of the CH bonds. As indicated in Table 5, there is for the isolated FDMEs molecules a larger σ^*(CH) occupation for the CH^g than for the CH^t bonds. These differences have been explained by the lone-pair effect, which results in a larger delocalization from the O lone pairs to the CH^g bonds.[16] The results of the present work show that, in agreement with this effect, there is in the isolated FDMEs a larger intramolecular hyperconjugation from the O lone pair to the $\sigma^*(CH^g)$ than to the $\sigma^*(CH^t)$ orbitals. In the CH_3OCH_3, CH_3OCH_2F, and CH_2FOCH_2F complexes where the O_wH_w···O1 hydrogen bond is predominating, the decrease of the hyperconjugation is larger for the CH^g than for the CH^t bonds. In these complexes, there is a small increase of the *s*-character of the C atom. For the cyclic complexes, our calculations predict a moderate decrease of the intramolecular

TABLE 3: MP2/6-311++G(d,p) Calculated ν(CH) Stretching Frequencies (cm^{-1}) and IR Intensities (km mol^{-1}) in Isolated FDMEs Isotopomers and the Complexes with Water

System	Free FDME		FDME−H_2O Complexes		Shift	
	$\nu(CH)^t$	$\nu(CH)^g$	$\nu(CH)^t$	$\nu(CH)^g$	$\Delta\nu(CH)^t$	$\nu(CH)^g$
CH_3OCH_3	3180(26)	3072(57)	3186(17)	3098(50)	+6	+26
CH_3OCH_2F	3195(32)	3096(59)	3200(16)	3115(50)	+5	+19
CH_2FOCH_2F(A)	3210(33)	3163(25)	3225(6)	3171(22)	+15	+8
CH_2FOCH_2F(B)	3210(33)	3163(25)	3244(4)	3161(28)	+34	−2
CH_3OCHF_2(A)	3227(30)		3247(7)		+20	
CH_3OCHF_2(B)	3227(30)		3265(2)		+38	
CH_3OCF_3	3220(9)	3172(14)	3227(3)	3179(13)	+7	+7
CH_2FOCHF_2(A)	3237(25)		3273(6)		+36	
CH_2FOCHF_2(B)	3237(25)		3269(5)		+32	
CHF_2OCHF_2	3248(18)		3280(2)		+32	
CH_2FOCF_3 (A)	3217(17)	3182(15)	3242(13)	3186(15)	+25	+4
CH_2FOCF_3 (B)	3217(17)	3182(15)	3247(2)	3180(14)	+30	−2
CHF_2OCF_3	3206(15)		3232(13)		+26	

TABLE 4: MP2/6-311++G(d,p) Calculated r(OH) Distances (Å), ν(OH) Vibrational Frequencies (cm^{-1}) and IR Intensities (km mol^{-1}, in Parentheses), Frequency Shifts and Ratio of the IR Intensities in the Complexes between FDMEs and H_2O

FDME−H_2O	$r(OH_w')^a$	$r(OH_w)$	$\nu^{as}(OH)^b$	$\nu^s(OH)$	$\Delta\nu(OH)^c$	$R(I^{as}/I^s)^d$
CH_3OCH_3	0.9687	0.9583	3968(100)	3732(458)	101	0.22
CH_3OCH_2F	0.9652	0.9585	3973(118)	3806(267)	58	0.44
CH_2FOCH_2F(A)	0.9631	0.9587	3981(123)	3840(97)	39	1.3
CH_3OCHF_2(A)	0.9630	0.9587	3983(119)	3843(79)	36	1.5
CH_3OCF_3	0.9623	0.9589	3985(122)	3855(60)	29	2.0
CH_2FOCHF_2(A)	0.9613	0.9593	3989(100)	3867(23)	21	4.3
CHF_2OCHF_2	0.9611	0.9593	3992(92)	3871(18)	18	5.1
CH_2FOCF_3(A)	0.9612	0.9592	3991(100)	3869(20)	19	5.0
CH_2FOCF_3(B)	0.9601	0.9589	3993(96)	3877(19)	16	5.1
CHF_2OCF_3	0.9603	0.9601	3992(94)	3875(18)	16	5.2

[a] The OH distance in isolated H_2O is 0.9589 Å. [b] The ν(OH) frequencies and IR intensities in isolated H_2O are 4008 cm^{-1} (63 km mol^{-1}) and 3889 cm^{-1} (12 km mol^{-1}). [c] Calculated from the average of the ν^{as}(OH) and ν^s(OH) frequencies. [d] Ratio of the IR intensities of the ν^{as}(OH) and ν^s(OH) vibrations.

TABLE 5: σ^*(CH) Population (me) and %*s*-Character of the C(H) in Isolated and Complexed FDMEs, %*s*-Character of the C (H) in Isolated FDMEs and Changes Resulting from the Interaction;[a] Results from B3LYP/6-311++G(d,p) Calculations

bond	σ^*(CH)°	σ^*(CH)°	$\Delta\sigma^*$(CH)/(OH_w)[b]	%*s*(C)°	%*s*(C)[c]	Δ%*s*(C)
CH_3OCH_3						
C2H4	10.2	9.1	−1.1	25.61	25.76	0.15
C2H5	23.3	20.2	−3.1	25.99	26.23	0.24
OH_w			22.7			
CH_3OCH_2F						
C3H8	27.0	25.8	−1.2	27.31	27.63	0.32
C3H9	39.7	37.0	−2.7	27.61	27.76	0.15
OH_w			13.6			
$CH_2FOCH_2F(A)$						
C3H7	25.7	24.4	−1.3	27.63	28.19	0.66
C3H9	31.6	30.3	−1.3	28.21	28.16	−0.05
OH_w			7.4			
$CH_2FOCH_2F(B)$						
C3H7	25.7	26.7	1.0	27.53	28.87	1.30
$CH_3OCHF_2(A)$						
C2H5	14.3	13.9	−0.4	26.70	26.77	0.07
C3H7	44.4	41.9	−2.5	29.43	30.21	0.78
OH_w			6.6			
$CH_3OCHF_2(B)$						
C2H5	14.3	14.8	0.5	26.70	26.65	−0.05
C3H7	44.4	42.8	−1.6	29.43	30.80	1.37
CH_3OCF_3						
C3H7	8.4	8.2	−0.2	25.86	26.47	0.61
C3H8	14.0	12.8	−1.2	26.73	26.70	−0.03
OH_w			5.0			
$CH_2FOCHF_2(A)$						
C2H4	28.4	27.86	−0.6	28.45	28.54	0.09
C3H7	42.5	41.4	−1.1	29.73	30.68	0.95
OH_w			2.6			
$CH_2FOCHF_2(B)$						
C2H4	28.4	28.6	0.2	28.45	28.40	−0.05
C3H7	42.5	43.4	0.9	29.73	31.20	1.47
CHF_2OCHF_2						
C3H7	43.7	41.2	−2.5	29.92	31.11	1.19
OH_w			1.1			
$CH_2FOCF_3(A)$						
C3H7	26.6	25.5	−1.1	27.63	28.56	0.93
C3H9	28.6	28.2	−0.4	28.38	28.23	−0.15
OH_w			1.9			
$CH_2FOCF_3(B)$						
C3H7	26.6	28.2	+1.6	27.63	29.05	1.42
CHF_2OCF_3						
C3H8	46.9	47.1	0.2	30.31	32.03	1.72
OH_w			0.9			

[a] The bold characters indicate the CH bond involved in the interaction. [b] The σ^*(OH) occupation in isolated H_2O is negligible.

hyperconjugation for both CH^g and CH^t bonds. It must be mentioned that for these complexes the intermolecular hyperconjugation energies $LPO_w \rightarrow \sigma^*$(CH) are somewhat larger than the intramolecular ones.

As suggested by the contractions of the CH bond, the increase of the ν(CH) frequencies and the decrease of the corresponding IR intensities, the B complexes, and the $CHF_2OCF_3 \cdot H_2O$ complex can be considered as *typical blue-shifted hydrogen bonds*. Complex formation results in an increase of the σ^*(CH) occupation (CH_2FOCH_2F, CH_2HOCHF_2, CH_2FOCF_3) and a decrease of the σ^*(CH) occupation (CH_3OCHF_2 and CHF_2OCF_3). In these five systems, there is an increase of the *s*-character of the carbon atom of the CH bond by 1.3 to 1.7%. These results suggest that, in the present cases, the rehybridization is the main factor contributing to the blue shift of the ν(CH) vibration.

We want now to discuss the effect of acidity and basicity of the ethers on the intermolecular hyperconjugation energies from the O_w lone pairs of water to the σ^*(CH) orbitals ($E^{(2)}$[$LPO_w \rightarrow \sigma^*$(CH)]. As expected, these hyperconjugation energies are the largest for the B complexes and for the CHF_2OCF_3 complexes where the molecules are held together by $CH\cdots O_w$ hydrogen bonds. They are comprised between 12.8 and 22.7 kJ mol^{-1} and are correlated to the acidity of the CH bonds involved in the interaction. For the A structures, the hyperconjugation energies are much lower, between 1.8 and 17.7 kJ mol^{-1}, owing to the simultaneous presence of the $O_wH_w\cdots O1$ hydrogen bonds. A plot of the $E^{(2)}$ energies

as a function of the DPE values shows a great scatter of the points. A closer inspection of our results suggests that the *effective* DPE becomes larger when the PA increases. In other words, when the CH bond becomes more acidic, the influence of the basicity of the O atom is lower. Our calculations show that, for the cyclic structures, the effective DPE is equal to DPE + 0.28 PA. These considerations allow one to derive a correlation involving the data for both the open and the cyclic structures. This correlation is illustrated in Figure 6:

$$E^{(2)}[LPO_w \rightarrow \sigma^*(CH)] = (9 \times 10^{-5})X^2 - 0.363X + 369 \quad (r = 0.992) \quad \textit{where} \quad X = DPE + 0.28PA \quad (kJmol^{-1}) \quad (6)$$

Eqs 5 and 6 indicate the reciprocal influence of the acidity and basicity of the proton donor and proton acceptor molecules involved in a hydrogen-bonded cyclic structure. The coefficients

TABLE 6: Intramolecular and Intermolecular Hyperconjugation Energies ($E^{(2)}$ in kJ mol^{-1}) in Isolated FDMEs and H_2O Complexes, Charge Transfer (CT) from FDMEs to H_2O (me), Differences between the NBO Charges on the H_w and $H_{w'}$ Atoms (me); Results from B3LYP/6-311++G(d,p) Calculations Using the MP2 Optimized Geometries

System[a]	$E^{(2)intra}$		$\Delta E^{(2)intra}$	$E^{(2)interm}$	CT[b]	$qH_w - qH_{w'}$[c]
	monomer	complex				
$CH_3OCH_3 \cdot H_2O$					21.1	25.8
LPO1 → σ*(C2H4)	10.2	9.1	−1.1			
LPO1 → σ*(C2H5)	30.6	25.9	−5.2			
LPO1 → σ*(O_wH_w)				37.7		
$CH_3OCH_2F \cdot H_2O$					12.2	25.5
LPO1 → σ*(C3H8)	11.6	11.	−0.6			
LPO1 → σ*(C3H9)	28.1	25.3	−2.8			
LPO1 → σ*(O_wH_w)				23.1		
$CH_2FOCH_2F \cdot H_2O(A)$					6.2	17.2
LPO1 → σ*(**C3H7**)	11.4	10.4	−1.0			
LPO1 → σ*(C3H9)	23.2	21.7	−1.6			
LPO1 → σ*(O_wH_w)				11.0		
LPO_w → σ*(**C3H7**)				2.1		
$CH_2FOCH_2F \cdot H_2O(B)$					−4.7	
LPO1 → σ*(**C3H7**)	11.4	9.7	−1.7			
LPO_w → σ*(**C3H7**)				12.8		
$CH_3OCHF_2 \cdot H_2O(A)$					5.8	16.4
LPO1 → σ*(**C3H7**)	12.0	10.9	−1.1			
LPO1 → σ*(C2H6)	23.4	22.6	−0.8			
LPO1 → σ*(O_wH_w)				9.1		
LPO_w → σ*(**C3H7**)				3.0		
$CH_3OCHF_2 \cdot H_2O(B)$					−5.4	
LPO1 → σ*(**C3H7**)	12.0	10.2	−1.8			
LPO1 → σ*(C2H6)	23.4	23.8	0.5			
LPO_w → σ*(C**3H7**)				15.3		
$CH_3OCF_3 \cdot H_2O$					3.9	14.4
LPO1 → σ*(**C3H7**)	9.3	8.5	−0.8			
LPO1 → σ*(C3H8)	20.8	19.5	−1.3			
LPO1 → σ*(O_wH_w)				7.3		
LPO_w → σ*(C3H7)				1.5		
$CH_2FOCHF_2 \cdot H_2O(A)$					1.0	8.5
LPO1 → σ*(C2H4)	14.2	13.4	−0.8			
LPO1 → σ*(**C3H7**)	11.7	10.3	−1.4			
LPO1 → σ*(O_wH_w)				1.7		
LPO_w → σ*(**C3H7**)				2.2		
$CH_2FOCHF_2 \cdot H_2O(B)$					−6.5	
LPO_w → σ*(**C3H7**)				17.6		
$CHF_2OCHF_2 \cdot H_2O$					−1.5	7.3
LPO1 → σ*(C2H6)	11.4	12.0	0.6			
LPO1 → σ*(**C3H7**)	11.5	10.0	−1.5			
LPO1 → σ*(O_wH_w)				0.9		
LPO_w → σ*(**C3H7**)				6.8		
$CH_2FOCF_3 \cdot H_2O(A)$					−0.1	8.7
LPO1 → σ*(**C3H7**)	12.5	10.9	−1.6			
LPO1 → σ*(C3H9)	14.9	14.4	−0.5			
LPO1 → σ*(O_wH_w)				2.1		
LPO_w → σ*(**C3H7**)				4.6		
$CH_2FOCF_3 \cdot H_2O$ (B)					−5.8	
LPO1 →σ(C3H7)*	12.5	10.4	−2.1	15.8		
LPO_w→ σ(C3H7)*						
$CHF_2OCF_3 \cdot H_2O$					−7.8	
LPO1 → σ*(C3H8)	20.8	19.5	−1.3			
LPO_w → σ*(C3H8)				23.2		

[a] The CH bonds in bold characters refer to the bonds involved in the interaction with H_2O. [b] Positive sign indicates CT from FDMEs to H_2O. [c] The NBO charges on the O and H atoms of isolated H_2O are −0.9088 and 0.4544 e. In the linear CH···O_w complexes, the difference $qH_w - qH_{w'}$ is negligible.

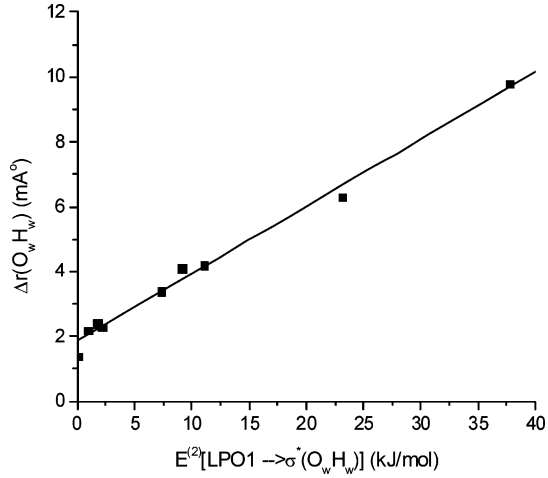

Figure 4. $\Delta r(O_wH_w)$ (mÅ) as a function of [$E^{(2)}$ (LPO1 → σ *(O_wH_w)] (kJ mol^{-1}).

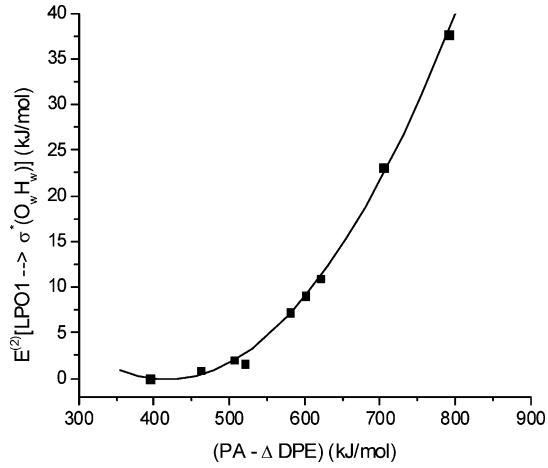

Figure 5. $E^{(2)}$ [LPO1 → σ*(O_wH_w)] (kJ mol^{-1}) as a function of (PA − ΔDPE) (kJ mol^{-1}).

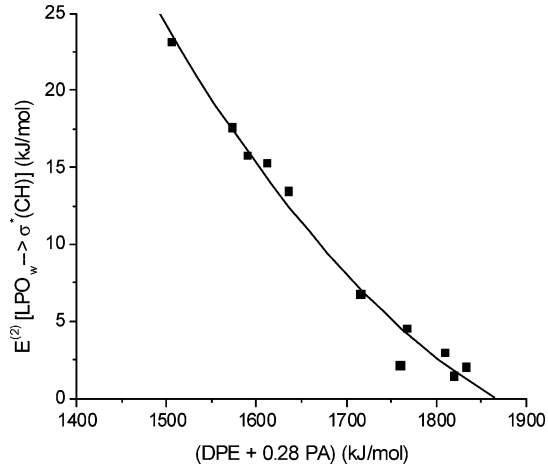

Figure 6. $E^{(2)}$ [LPO_w → σ*(CH)] (kJ mol^{-1}) as a function of (DPE + 0.28 PA) (kJ mol^{-1}).

of the second-order polynomial (5) and (6) are valuable for the present systems but are expected to be different for other closed structures.

For the most stable complexes, the charge transfer is moderate (4 to 21 me) and takes place from the FDMEs to the H_2O molecules. When the number of F atoms is larger than three, the charge transfer is nearly zero. For the linear complexes, the lowest value of the charge transfer from H_2O to the FDMEs (4.7 me) is predicted for the CH_2FOCH_2F complex where the CH bond has the lowest acidity and the largest value of the charge transfer (7.8 me) is obtained for the CHF_2OCF_3 complex where the CH bond is characterized by the largest acidity.

Finally, we want to add a few words on the competition between the $O_wH_w\cdots O$ and $CH\cdots O_w$ hydrogen bonds in the closed structures. A comparison of the parameters discussed in the present work suggests than the energy of the $O_wH_w\cdots O$ and $CH\cdots O_w$ hydrogen bonds in the $CH_2FOCHF_2\cdot H_2O$ complex is about the same. For this complex, our calculations show that there is a marked drop in the frequency shift of the ν(OH) vibration and the ratio of the IR intensities $\nu^{as}(OH)/\nu^{s}(OH)$. Further the $E^{(2)}$[(LPO1 → σ*(O_wH_w)] and $E^{(2)}$[LPO_w → σ*(CH)] hyperconjugation energies are about the same, respectively 1.7 and 2.2 kJ mol^{-1}. In the $CH_3OCF_3\cdot H_2O$ complex, the first hyperconjugation energy is much larger than the second one and the reverse holds for the $CHF_2OCHF_2\cdot H_2O$ system.

Conclusions

In the present work, the interaction between dimethyl ether and fluorinated dimethyl ethers ($n_F = 1-5$) and water is investigated by theoretical methods. Important conclusions are the following ones:

1. When $n_F = 0, 1$, the hydrogen bonds are formed on the O atom of the ethers. When $n_F = 5$, the CH bond of the ether derivative acts a proton donor forming a $CH\cdots O_w$ hydrogen bond. When $n_F = 2-4$, the most stable structures are cyclic and stabilized by both $O_wH_w\cdots O$ and $CH\cdots O_w$ hydrogen bonds. The binding energies range between −4 and −12 kJ mol^{-1}.

2. The ν(CH) vibrations are blue-shifted even when the CH bond is not involved in the interaction.

3. The vibrational data and the NBO parameters clearly show the differences between $O_wH_w\cdots O$ and $CH\cdots O_w$ hydrogen bonds.

4. The theoretical results are discussed as a function of the acidity of the CH bonds and the basicity of the O atom of the fluorinated dimethyl ethers. It is shown that the effective proton affinity of the O atom of the ethers in determining the LPO_w → σ*(CH) hyperconjugation energies decreases with increasing acidity of the CH bond. In turn, the effective acidity of the CH bond in determining the LPO_w → σ*(CH) hyperconjugation energies decreases with increasing basicity of the ethers.

Acknowledgment. A.K.C. thanks DST, India, for financial support through a research project (SR/S1/PC-13/2005) and UGC, India, for their support through special assistance program.

Supporting Information Available: Other stable structures of complexes between FDMEs and water, NBO charges on all the atoms for the complexes discussed in the present work. This material is available free of charge via the Internet at http://pubs.acs.org.

References and Notes

(1) (a) Scheiner, S. *Hydrogen Bonding*; Oxford University Press: New York, 1997. (b) Jeffrey, G. A. *An Introduction to Hydrogen Bonding*; Oxford University Press: New York, 1997.

(2) Desiraju, G. R. *Crystal Engineering, The Design of Organic Solids*; Elsevier: Amsterdam, 1989.

(3) Staikova, M.; Donaldson, D. J. *Phys. Chem. Chem. Phys.* **2001**, *3*, 1999.

(4) *Hydrogen Bonding: New Insights*; Grabowski, S. J. Ed.; Springer: New York, 2006.

(5) Theoretical studies of blue-shifted hydrogen bonds:See for example: (a) Wetmore, S. D.; Schofield, R.; Smith, D. M.; Radom, L. *J.*

Phys. Chem. A **2001**, *105*, 8718. (b) Li, X.; Liu, L.; Schlegel, H. B. *J. Am. Chem. Soc.* **2002**, *124*, 9639. (c) Alonso, J. L.; Antolines, S.; Blanco, A.; Lesarri, A.; Lopez, J. C.; Carminati, W. *J. Am. Chem. Soc.* **2004**, *126*, 3244. (d) McDowell, S. A. C.; Buckingham, A. D. *J. Am. Chem. Soc.* **2005**, *127*, 15515. (e) Yang, Y.; Zhang, W.; Gao, X. *Int. J. Quantum Chem.* **2006**, *106*, 1199. (f) Desiraju, G. R. *Acc. Chem. Res.* **2002**, *35*, 565. (g) Hobza, P.; Havlas, Z. *Theor. Chem. Acc.* **2002**, 108–325. (h) Hobza, P.; Havlas, Z. *Chem. Rev.* **2000**, *100*, 4253. (i) Masunov, A.; Dannenberg, J. J.; Contreras, R. H. *J. Phys. Chem. A* **2001**, *105*, 4737. (ii) Kryachko, E. S.; Zeegers-Huyskens, Th. *J. Phys. Chem. A* **2001**, *105*, 7118. (j) Nguyen, H. M. T.; Nguyen, M. T.; Peeters, J.; Zeegers-Huyskens, Th. *J. Phys. Chem. A* **2004**, *108*, 11101.

(6) Experimental studies of the blue-shifted hydrogen bonds, see for example: (a) Rutkowski, K. S.; Rodziewicz, P.; Melikova, S. M.; Koll, A. *ChemPhysChem* **2005**, *6*, 1282. (b) Katsumoto, H.; Kamatsu, H.; Ohno, K. *J. Am. Chem. Soc.* **2006**, *128*, 9278. (c) Delanoye, S. N.; Herrebout, W. A.; Van der Veken, B. J. *J. Am. Chem. Soc.* **2002**, *124*, 7490. (d) Rutkowski, K. S.; Rodziewicz, P.; Melikova, S. M.; Herrebout, W. A.; Van der Veken, B. J.; Koll, A. *Chem. Phys.* **2005**, *313*, 225. (e) Matsuura, H.; Yoshida, H.; Hieda, M.; Yamanaka, S.; Harada, T.; Shin-ya, K.; Ohno, K. *J. Am. Chem. Soc.* **2003**, *125*, 13910. (f) Dozova, N.; Krim, L.; Alikani, M. E.; Lacome, N. *J. Phys. Chem. A* **2007**, *111*, 10055. (g) Michalska, D.; Bieňko, D. C.; Czarnik-Matusewicz, B.; Wierzejwska, M.; Sandorfy, C.; Zeegers-Huyskens, Th. *J. Phys. Chem. B* **2007**, *111*, 12238.

(7) (a) Gu, Y.; Kar, T.; Scheiner, S. *J. Am. Chem. Soc.* **1999**, *121*, 9411. (b) Kar, T.; Scheiner, S. *J. Phys. Chem. A* **2004**, *108*, 9191.

(8) Alabugin, I. V.; Manoharan, M.; Peabody, S.; Weinhold, F. *J. Am. Chem. Soc.* **2003**, *125*, 5973.

(9) (a) Hermansson, K. *J. Phys. Chem. A* **2002**, *106*, 4695. (b) Pejov, L.; Hermansson, K. *J. Chem. Phys.* **2003**, *119*, 313.

(10) Joseph, J.; Jemmis, E. D. *J. Am. Chem. Soc.* **2007**, *129*, 4620.

(11) Udagawa, T.; Ishimoto, T.; Tokiwa, H.; Tachikawa, M.; Nagashima, U. *J. Phys. Chem. A* **2006**, *110*, 7279.

(12) (a) Clotman, D.; Van Lerberghe, D.; Zeegers-Huyskens, T. *Spectrochim. Acta* **1970**, *264*, 1621–1631. (b) Zeegers-Huyskens, T.Thèse d'Aggrégation de l'Enseignement Supérieur, Université Catholique de Louvain, 1970. (c) Barnes, A. J.; Beech, T. R. *Chem. Phys. Lett.* **1983**, *94*, 568. (d) Vanderheyden, L.; Maes, G.; Zeegers-Huyskens, Th. *J. Mol. Struct.* **1984**, *114*, 568. (e) Xu, Z.; Li, H.; Wang, C.; Wu, Y. T.; Han, S. *Chem. Phys. Lett.* **2004**, *394*, 405.

(13) (a) Bohlmann, F. *Chem. Ber.* **1958**, *91*, 2157. (b) Bohlmann, F. *Angew. Chem.* **1975**, *69*, 641. (c) Ernstbrunner, E.; Hudec, J. *J. Mol. Struct.* **1974**, *17*, 249.

(14) (a) Wiberg, K. B.; Marquez, M.; Castejon, H. *J. Org. Chem.* **1994**, *59*, 6817. (b) Pophristic, V.; Goodman, L.; Guchhait, N. *J. Phys. Chem. A* **1997**, *101*, 4290.

(15) (a) Chandra, A. K.; Parveen, S. Zeegers-Huyskens, Th. *J. Phys. Chem. A* **2007**, *111*, 8884–8891. (b) Chandra, A. K.; Parveen, S.; Das, S.; Zeegers-Huyskens, Th. *J. Comput. Chem.* **2008**, *29*, 1490. (c) Zeegers-Huyskens, Th. *J. Mol. Struct.* **2008**, *887*, 2. (d) Parveen, S.; Das, S.; Chandra, A.; Zeegers-Huyskens, T. *J. Theor. Comput. Chem.* **2008**, *7*, 1171.

(16) Nam, P. C.; Nguyen, M. T.; Zeegers-Huyskens, Th. *J. Mol. Struct. Theochem* **2007**, *821*, 71.

(17) (a) Barnes, A. J.; Beech, T. R. *Chem. Phys. Lett.* **1983**, *94*, 568. (b) van der veken, B. J.; Herrebout, W. A.; Szostak, R.; Shchepkin, D. M.; Havlas, Z.; Hobza, P. *J. Am. Chem. Soc.* **2001**, *123*, 12290. (c) Vijayakamur, S.; Kolandaivel, P. *J. Mol. Struct.* **2004**, *734*, 157. (d) Urata, S.; Tsuzuki, S.; Takata, A.; Mikami, M.; Uchimaru, T.; Sekiya, A. *J. Comput. Chem.* **2004**, *25*, 447. (e) Herrebout, W. A.; Delanoye, S. N.; van der Veken, B. J. *J. Phys. Chem. A* **2004**, *108*, 6059. (f) Van den Kerkhof, T.; Bouwen, A.; Goovaerts, E.; Herrebout, E.; van der Veken, B. *Phys. Chem. Chem. Phys.* **2004**, *6*, 358. (g) Herrebout, W. A.; Delanoye, S. N.; Maes, B. U. W.; van der Veken, B. J. *J. Phys. Chem. A* **2006**, *110*, 13759.

(18) (a) Tatamitani, Y.; Liu, B.; Shimada, J.; Ogata, T.; Ottaviani, P.; Maris, A.; Caminati, W.; Alonso, J. L. *J. Am. Chem. Soc.* **2002**, *124*, 2739. (b) Bleiholder, C.; Werz, D. B.; Köppel, R.; Gleiter, R. *J. Am. Chem. Soc.* **2006**, *128*, 2666.

(19) Lee, C.; Yang, W. R. G.; Parr, R. G. *Phys. Rev. B* **1988**, *37 B*, 785.

(20) Reed, A. E.; L, A; Curtiss, L. A.; Weinhold, F. *Chem. Rev.* **1988**, *88*, 899.

(21) Boys, S. F.; Bernardi, F. *Mol. Phys.* **1970**, *19*, 553.

(22) Frisch, M. J.; Trucks, G. W.; Schlegel, H. B.; Scuseria, G. E.; Robb, M. A.; Cheeseman, J. A. Montgomery, T., Jr.; Vreven, T.; Kudin, J. C.; Burant, J. C.; Millam; J. M.; Iyengar, S. S.; Tomasi, J.; Barone, V.; Menucci, B.; Cossi, M.; Scalmani, G.; Rega, G. A.; Petersson, G. A.; Nakatsuji, H.; Hada, M.; Ehara, M.; Toyota, K.; Fukuda, R.; Hasegawa, J.; Ishida, M.; Nakajima, T.; Honda, Y.; Kitao, O.; Nakai, H.; Klene, M.; Li, X.; Knox, J. E.; Hratchian, H. P.; Cross, J. B.; Adamo, C.; Jaramillo, J.; Gomperts, R.; Stratmann, R. E.; Yazuev, O.; Austin, A. J.; Cammi, R.; Pomelli, C.; Ochterski, J. W.; Ayala, P. Y.; Morokuma, K.; Voth, G. A.; Salvator, P.; Dannenberg, J. J.; Zakrzewski, V. G.; Dapprich, S.; Daniels, A. D.; Strain, M. C.; Farkas, O.; Malick, D. K.; Rabuck, A. D.; Raghavachari, K.; Foresman, J. B.; Ortiz, J. V.; Cui, Q.; Baboul, S.; Cliford, S.; Ciolowski, J.; Stefanov, B. B.; Liu, G.; Liashenko, P.; Piskorz, P.; Komaromi, I.; Martin, R. L.; Fox, D. J.; Keith, T.; Al-Laham, M. A.; Peng, C. Y.; Nanayakkara, A.; Challacombe, M.; Gilli, P. M. W.; Johnson, B.; Chen, W.; Wong, M. W.; Gonzales, C.; Pople, J. A. *Gaussian 03*, Rev. B.03; Gaussian Inc.: Pittsburgh, PA, 2003.

(23) Karpfen, A.; Kryachko, E. *Chem. Phys. Lett.* **2006**, *431*, 428.

(24) Solimannejad, M.; Scheiner, S. *Chem. Phys. Lett.* **2006**, *429*, 38.

(25) NIST Chemistry WebBook, NIST Standard Reference Database, Number 69, June 2005.

(26) (a) Chandra, A. K.; Nguyen, M. T.; Uchimaru, T.; Zeegers-Huyskens, Th. *J. Phys. Chem. A* **1999**, *103*, 8853. (b) Kryachko, E. S.; Nguyen, M. T. Zeegers-Huyskens, Th. *J. Phys. Chem. A* **2001**, *105*, 1934. (c) Chandra, A. K.; Uchimaru, T. Zeegers-Huyskens, Th. *J. Mol. Struct.* **2002**, *615*, 213.

(27) (a) Kuhn, R.; Christen, D.; Mack, H. G.; Konikowski, D.; Minkwitz, R.; Oberhammer, H. *Chem. Phys. Lett.* **1996**, *259*, 287. (b) Pophristic, V.; Goodman, L.; Guchhait, N. *J. Phys. Chem. A* **1997**, *101*, 4290.

(28) (a) Kuhn, R.; Christen, D.; Mack, H. G.; Konikwoski, D.; Minkwitz, R.; Oberhammer, H. *J. Mol. Struct.* **1996**, *376*, 217. (b) Radice, S.; Toniolo, P.; Avatanio, M.; De Patto, U.; Marchionni, G.; Castiglioni, C.; Tommasini, M.; Zerbi, G. *J. Mol. Struct.* **2004**, *710*, 151.

(29) Huyskens, P. L.; Luck, W. A. P.; Zeegers-Huyskens, Th. *Intermolecular Forces, An Introduction to Modern Methods and Results*; Springer-Verlag: Berlin, Heidelberg, NY, 1991and references therein.

(30) (a) Zeegers-Huyskens, Th. *Chem. Phys. Lett.* **1986**, *129*, 172. (b) Zeegers-Huyskens, Th. *J. Org. Chem.* **1999**, *64*, 4946. (c) Bian, L. *J. Phys. Chem. A* **2003**, *107*, 11517. (d) Lankay, T.; Yu, C.-H. *Phys. Chem. Chem. Phys.* **2007**, *9*, 299. (e) Chan, B.; Del Bene, J. E.; Radom, L. *J. Am. Chem. Soc.* **2007**, *129*, 12197.

JP902244J